Published OnlineFirst January 20, 2017; DOI: 10.1158/1541-7786.MCR-16-0234

and the sequences are identical to those of Sigma-Aldrich Mission pLKO.1-puro vectors. Lentiviral particles were generated as described above and transduced into BJAB-LexR cells or MDA-MB231-TRAILR cells as described. As negative controls, nontargeting Mission pLKO.1-puro nontarget viral particles were generated and transduced to cells in parallel.

Cell culture

All cells were cultured at 37°C in humidified air supplemented with 5% CO_2. 293FT cells were cultured in DMEM and supplemented with 10% FBS and penicillin/streptomycin. MDA-MB-231 cells were cultured in DMEM supplemented with 5% FBS, insulin, Hepes, and nonessential amino acids (Sigma). BJAB lymphoma cells were cultured in RPMI1640 with 10% FBS. The SLC26A2 expression plasmid purchased from Addgene was a kind gift from Dr. Antonio Rossi (Department of Molecular Medicine, University of Pavia, Section of Biochemistry, Pavia, Italy; ref. 25).

Cell line authentication

The BJAB-wt and LexR cell lines and the MDA-MB-231 SEN and TRAIL R cells were recently profiled (07/2016) to confirm their identity.

qRT-PCR

cDNA synthesis was performed using the iScript Kit (Bio-Rad) from total RNA that was isolated using the RNAeasy Extraction Kit (Qiagen). qRT-PCR reactions were run using ssoFast Evagreen supermix (Bio-Rad) and primers for either *SLC26A2*, (AGCTCCAAGGGATCATGGGAAAGTTGC, CATACTCAGCTTTCTGGTGTGGTAACAGC), *DR4* (TGTACAATCACCGACCTTGACCA, AGCTAAGTCCCTGCACCACGA), *DR5* (TCCTGGACTTCCATTTCCTG, TGCAGCCGTAGTCTTGATTG), *CRKL*, *AGTR2*, *TBX2* (TTCCACAAACTGAAGCTGAC, GCTGTGTAATCTTGTCATTCTG), *GAPDH* (ACCCAGAAGACTGTGGATGG, TCTAGACGGCAGGTCAGGTC), or *18s* (ACCCGTTGAACCCCATTCGTGA, GCCTCACTAAACCATCCAATCGG) with the Bio-Rad CFX96.

Western blot analysis

Whole cell extracts were harvested from equal numbers of cells for all conditions tested. After lysates were sonicated, they were loaded onto acrylamide gels and electophoresed, after which they were transferred to PVDF membranes. After blocking in 5% milk in Tris-buffered saline with 0.1% tween (TBST) for 1 hour, membranes were incubated in primary antibodies overnight with constant rocking at 4°C. After washing in TBST, membranes were incubated in the appropriate HRP-conjugated secondary antibodies for 1 hour at room temperature with constant rocking. The primary antibodies used were SLC26A2 [(1:500, Novus Biologicals 3F6), DR4 (1:500, AbCam #ab8414)], DR5 (1:500, AbCam #ab8416), and β-actin (1:10,000, Sigma-Aldrich).

Cell viability assays

The number of viable cells in transduced and treated cells was assessed using the CellTiter-Glo Luminescent Cell Viability Assay (Promega), a luminescent assay that quantifies ATP which is directly proportional to the number of viable cells, per manufacturer's instructions. Cells were set up at 0.25×10^6 cells/mL in white 96-well plates and 24 hours later serial dilutions of reagents [recombinant TRAIL (Genentech), doxorubicin (Sigma), or etoposide(Sigma)] were added in triplicate. Cells were incubated for 24 hours, luminescence was assayed within 5 hours of adding the CellTiter-Glo using a using a Turner Biosystems Modulus Microplate reader.

Propidium iodine staining

To assess propidium iodine (PI) positive BJAB cells via flow cytometry, we utilized the FITC Annexin-V Apoptosis Detection Kit I (BD Biosciences #556547) according to manufacturer's instructions. Specifically, 0.25 cells/mL were washed with PBS solution and then resuspended in 1× binding buffer to 1×10^6 cells/mL. One hundred microliters of the cell solution was transferred to a culture tube and incubated with 5 μL of FITC-Annexin V and 5 μL of PI (although FITC-Annxin V was not used for the current analysis) for 15 minutes at room temperature in the dark. A total of 400 μL of 1× binding buffer was added to stained cells prior to analysis with a Beckman Coulter FC500. Cells that underwent heat shock at 42° for 1 hour were used as a positive control for dead cells for gating purposes.

Caspase-3/7 apoptosis assay

A total of 1,000 MDA-MB-231 cells were plated in replicates of six in 96-well plates. Twenty-four hours later, cells were treated with serial dilutions of TRAIL and 5 μmol/L CellEvent caspase 3/7 (Invitrogen C10423). Cells were monitored every 2 hours with live cell, *in vitro* microscopy imaging via Incucyte Zoom (Essen BioScience).

Flow cytometry

Equal numbers of cells for all conditions tested were harvested and spun down via centrifugation and then washed three times in PBS supplemented with 0.5% BSA. Cells were resuspended in 100 μL of Flow Cytometry Staining Buffer (PBS + 1 mmol/L EDTA + 25 mmol/L HEPES pH 7.0 + 1.0% FBS) per 1×10^6 cells and were blocked with 1 μg/1×10^6 cells of anti-mouse IgG (Fc specific) antibody (M4280, Sigma Aldrich) for 15 minutes at room temperature. 10 μL/1×10^6 of PE-conjugated antibodies against DR4 (FAB347P, R&D Systems) and DR5 (FAB6311P, R&D Systems) were then added and allowed to incubate for 30 minutes at room temperature in the dark followed by three washes with flow cytometry staining buffer. The X-median or the geometric mean for percent positive cells was then analyzed with a Beckman Coulter FC500 where populations were gated based on unstained samples for each condition.

Data mining

Publicly available data sets were examined using either Oncomine or KMplot.com. For data analyzed though oncomine, studies with a *P*-value of 0.05 or greater and a fold change of two or greater were reported. For data analyzed through KMplot (2014 version), probe set 205097_at was used to analyze *SLC26A2* expression in systemically untreated breast cancer patients, redundant samples were removed, unbiased data were excluded, and proportional hazards assumptions were checked. Results were split by the "auto select best cut off" and graphed such that the approximate bottom quartile are considered "low" expression and the remaining top three quartiles are considered "high" expression. Results are censored at threshold (26).

Micorarray gene expression data analysis

Parental and TRAIL-resistant MDA-MB-231 cells and WT BJAB and LEXR cells were treated with recombinant TRAIL at 100 ng/mL

Published OnlineFirst January 20, 2017; DOI: 10.1158/1541-7786.MCR-16-0234

for 2 hours. RNA was isolated using TRIzol (Thermo Fisher Scientific) and was further purified (including a gDNA removal step) using the RNeasy PLUS Micro Kit (Qiagen). Isolated RNA from these samples were hybridized on Affymetrix HuGene 1.0 ST microarrays according to manufacturer's manual (Affymetrix). Gene expressions were normalized by using the Robust Multiarray Average (RMA; ref. 27) method as previously described using Affymetrix Power Tool. Gene Set Enrichment Analysis (GSEA; ref. 28) was performed on the normalized data using KEGG gene sets. Raw microarray data have been deposited into NCBI Gene Expression Omnibus with GSE82047.

Pathway analysis

Genome-scale integrated analysis of gene networks (GIANT; ref. 29) was used with a confidence cut off of 0.5 and a maximum gene cut off of 20 across all tissue types.

Results

A genome-wide loss-of-function screen in a cell model of acquired TRAIL resistance

To perform a screen to identify novel mechanisms of TRAIL resistance, we selected the Burkitt lymphoma cell line, BJAB, which is inherently sensitive to TRAIL, and its TRAIL-resistant subline, LexR. The BJAB LexR subline was previously made resistant to TRAIL-induced apoptosis via increasing exposure to Lexatumumab, an agonistic antibody to the functional TRAIL receptor, TNF, and has been previously characterized to show a marked increase in cell growth in the presence of Lexatumumab as compared to parental counterparts, BJAB-wild-type (wt) cells (16). A cell viability assay confirmed that BJAB-LexR cells are significantly more resistant to TRAIL than are BJAB-wt cells (Fig. 1A). Importantly, this induced resistance is specific to the TRAIL pathway, as the BJAB-LexR cells do not show increased resistance to other apoptosis inducing chemotherapeutics including doxorubicin or etoposide (Supplementary Fig. S1A and S1B).

Using the BJAB system, we performed a genome-wide loss-of-function screen. To perform the screen, we introduced a library of lentiviral particles expressing shRNAs targeting the entire human genome to BJAB cells with forced resistance to LexR (BJAB-LexR) and then subjected the cells to either no treatment or TRAIL treatment (Fig. 1B). In this screen, over-representation of a particular shRNA after TRAIL treatment implies that the target gene promotes TRAIL-induced apoptosis and, conversely, an under-representation of a certain shRNA after TRAIL treatment implies that the target promotes resistance against TRAIL-induced apoptosis. As shown in Fig. 1C, there were clear differences in the representation of different shRNAs before and after TRAIL treatment, indicating that selection of certain shRNAs has, in fact, taken place. After analysis of the altered shRNAs in the BJAB-LexR TRAIL–treated and untreated cells, we identified 580 candidate resistance genes that were within the statistical cut-off, $E < 2$. We selected 182 candidates from this gene list, and constructed a secondary library consisting of pooled shRNAs (2 to 5 shRNAs per gene) specifically targeting these genes. The top candidates confirmed in this secondary screen were then validated using specific shRNAs. We confirmed that knockdown (KD) of Angiotensin II Receptor 2 (AGTR2), Crk-like protein (CRKL), T-Box Transcription Factor 2 (TBX2), and solute carrier family 26 (anion exchanger), member 2 (SLC26A2) in LexR cells (Fig. 2A–D) significantly reduced TRAIL resistance (Fig. 2E–H) with the reduction of resistance correlating to the level of KD seen with the two shRNAs.

Novel TRAIL-resistant genes identified in a lymphoma model also mediate resistance in breast cancer

Next, we asked whether the effects of AGTR2, CRKL, TBX2, and SLC26A2 on TRAIL resistance were unique to BJAB cells or if similar results could be observed in other tumor types. To this end, we developed a similar model of TRAIL resistance in MDA-MB-231 breast cancer cells through long-term exposure to increasing concentrations of a recombinant TRAIL ligand, generating a TRAIL-resistant subline, 231-TRAILR. 231-TRAILR cells are resistant to TRAIL specifically, but are not generally resistant to apoptosis because they retain sensitivity to doxorubicin and etoposide, similar to that of the parental cells (Fig. 3A; Supplementary Fig. S2A and S2B). In concordance with what we found in the BJAB-LexR system, knocking down AGTR2, CRKL, TBX2, and SLC26A2 (Fig. 3B–E), all rendered the MDA-MB-231-TRAILR breast cancer cells significantly more sensitive to TRAIL-induced apoptosis (Fig. 3F–I).

Of the genes identified, the sulfate transporter, *SLC26A2*, had the most robust effect when assessed across both systems. This gene is understudied in the context of cancer or drug resistance, and thus we decided to pursue it further. To better explore the mechanism by which SLC26A2 mediates resistance in breast cancer cells, we established clonal isolate sublines of the 231-TRAILR line with stable KD of SLC26A2 expression using two different shRNA constructs. shRNA1 (sh1) targets *SLC26A2* in the 3′UTR of the gene, whereas shRNA2 (sh2) targets the coding region. KD of SLC26A2 with either of these constructs selectively enhanced TRAIL sensitivity in 231-TRAILR cells, but did not affect sensitivity to other general chemotherapeutics including doxorubicin and etoposide (Fig. 4A and B; Supplementary Fig. S3A and S3B). As a test of the specificity of the KD, we rescued SLC26A2 expression with a construct containing only the coding sequence. This construct restored TRAIL resistance in the cells expressing the shRNA1 KD because it lacks the 3′UTR and thus is resistant to shRNA1 KD, but did not restore resistance in cells expressing the shRNA2 construct that targets the coding region (Fig. 4A and B), thus demonstrating that the KD of SLC26A2 is sequence-specific. Taken together, these data demonstrate that SLC26A2 is a novel mediator of TRAIL resistance.

KD of SLC26A2 leads to enhanced expression of DR4 and DR5

To determine if the increase in viability observed with SLC26A2 KD in LEXR cells was due to cell death, we stained BJAB-LEXR cells with PI, a nuclear stain that is excluded by live cells and therefore indicative of late-apoptotic or necrotic cells. Uptake of PI, corresponding to cell death was quantified by flow cytometry. Cell death was dramatically increased in both BJAB-SLC26A2 KD lines as compared to the nontargeting control line (Fig. 5A). In the adherent MDA-MB-231 cell lines, we performed an activated-caspase 3/7 assay by measuring green fluorescence with Incucyte live cell imaging after the addition of CellEvent caspase-3/7 and TRAIL. Indeed, we observed a significant increase in activated caspase 3/7 in the MDA-MB-231 TRAILR SLC26A2 KD lines as compared to the nontargeting control (Fig. 5B). Taken together,

Published OnlineFirst January 20, 2017; DOI: 10.1158/1541-7786.MCR-16-0234

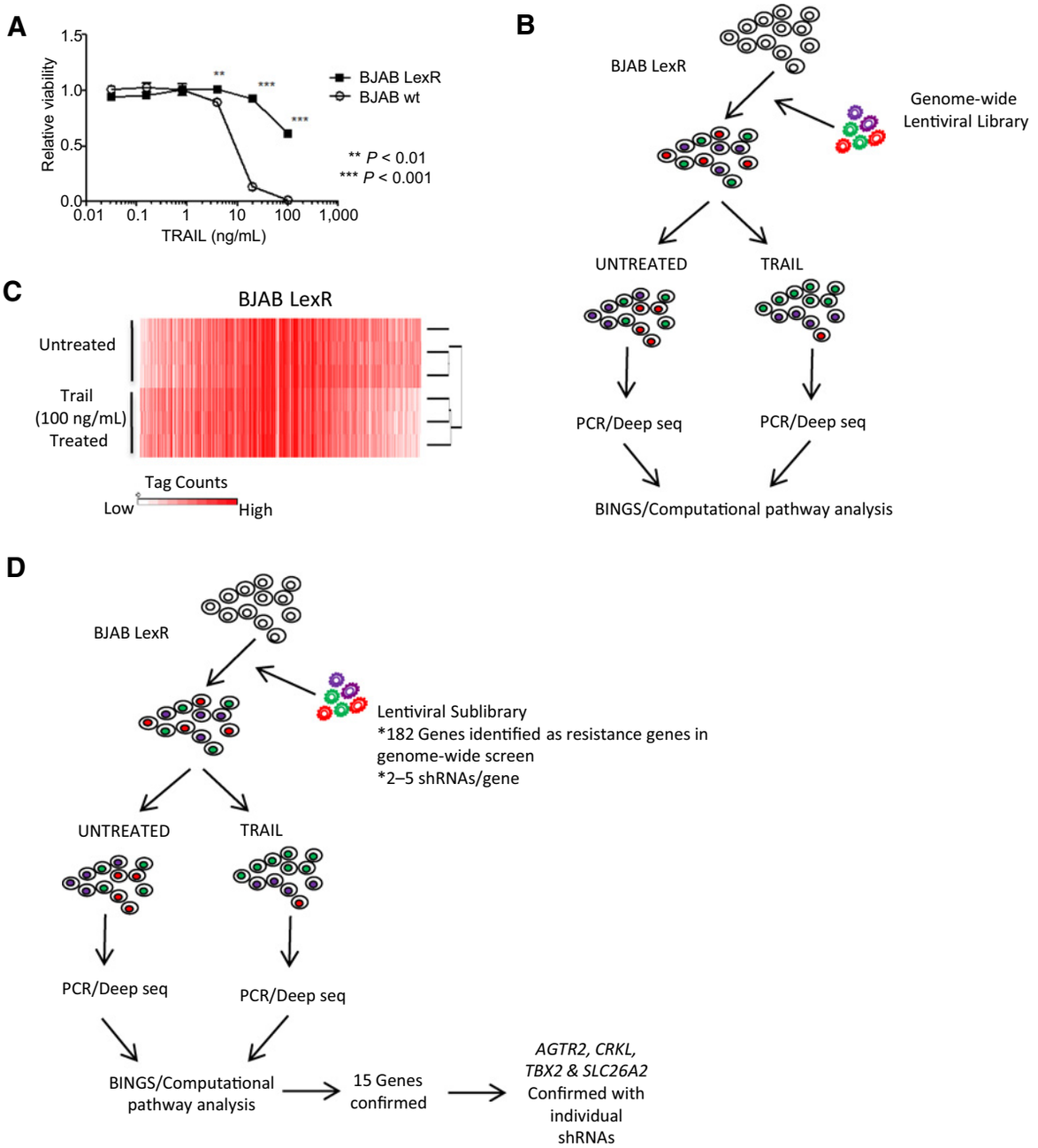

Figure 1.

Genome-wide loss-of-function shRNA screening of a TRAIL-resistant lymphoma cell line. Lymphoma cell lines BJAB-LexR (TRAIL resistant) were treated with indicated concentrations of recombinant TRAIL for 24 hours (**A**). Relative viability compared with untreated cells was determined by CellTiter 96 AQueous Non-Radioactive Cell Proliferation Assay. Representative experiments are shown (of ≥3 experiments) with each experiment performed in triplicate. Statistical significance assessed by two-way ANOVA with a Bonferroni posttest. **B,** Schematic of shRNA screen: BJAB-LexR cells were transduced with a genome-wide lentiviral shRNA library and treated with recombinant TRAIL (100 ng/mL) for 24 hours. **C,** RNA was extracted after transduction with the shRNA library and pre- and post-treatment with TRAIL and analyzed by deep sequencing. Results show clear differences in the shRNA representation between untreated and TRAIL-treated BJAB-LexR cells. **D,** Schematic of secondary shRNA screen: BJAB-LexR cells were treated with a lentiviral shRNA sublibrary and treated with recombinant TRAIL (100 ng/mL) for 24 hours. Hits confirmed from the primary and secondary screens were then individually tested with individual shRNAs.

these results indicate that the decrease of viable cells observed with loss of SLC26A2 is due to increased apoptosis in TRAIL-resistant cell lines.

To understand mechanistically how SLC26A2 could affect cell death, we performed gene expression analysis in the MDA-MB-231 SENS and TRAILR cell lines and

Published OnlineFirst January 20, 2017; DOI: 10.1158/1541-7786.MCR-16-0234

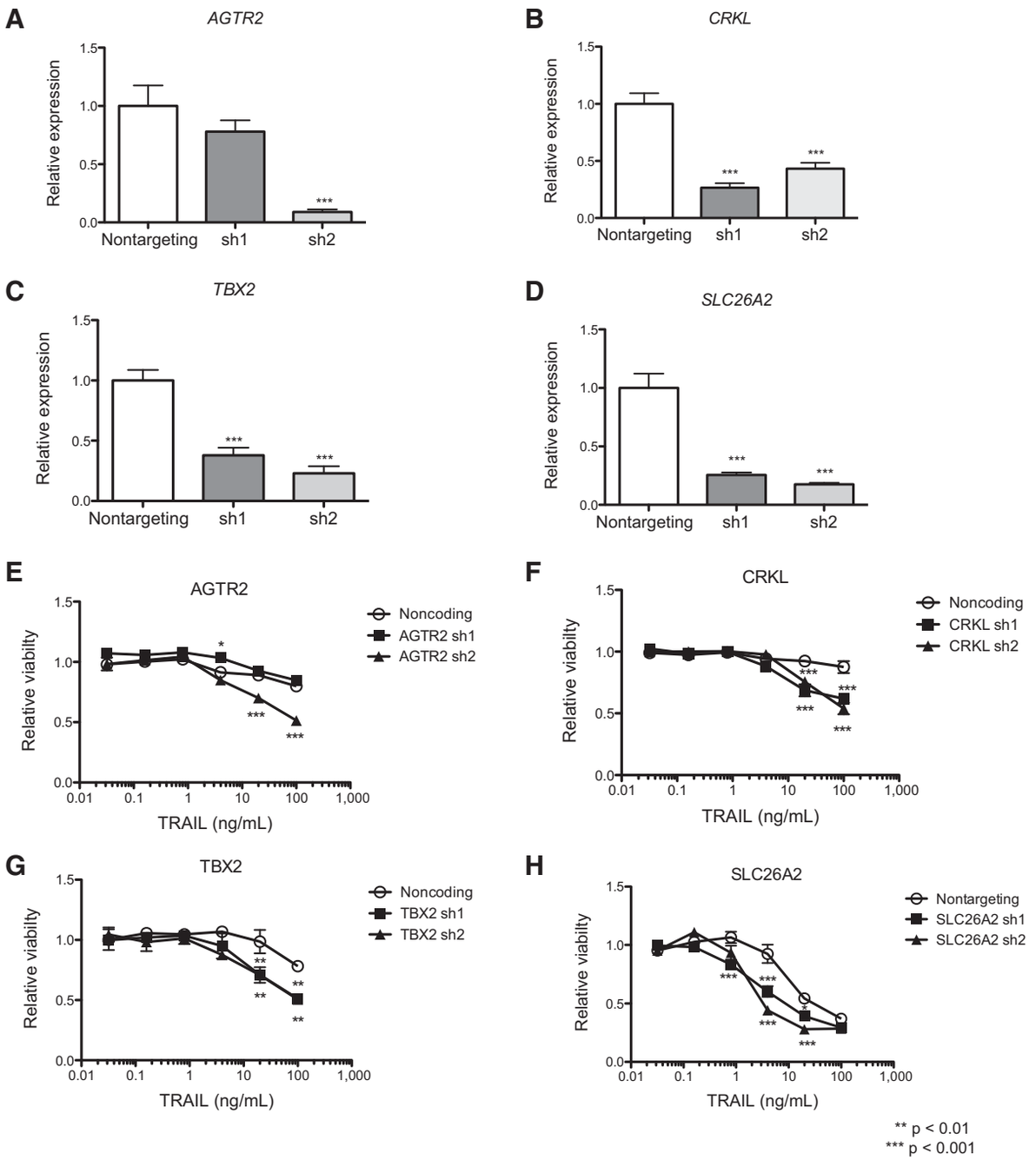

Figure 2.

AGTR2, CRKL, TBX2, and SLC26A2 mediate resistance to TRAIL in BJAB cells. TRAIL-resistant BJAB-LexR cells were lentivirally transduced with either a control, nontargeting shRNA vector (nontargeting) or with either of two different individual shRNAs (sh1, sh2) targeting *AGTR2* (**A**), *CRKL* (**B**), *TBX2* (**C**), and *SLC26A2* (**D**). KD was determined by qRT-PCR. The expression is relative to the expression of GAPDH and was normalized to nontargeting *shRNA* vector-expressing cells. Representative experiments are shown (of ≥3 experiments) with each experiment performed in triplicate. Statistical significance assessed by two-way ANOVA with a Bonferroni posttest. (**E-H**) BJAB-LexR cells transduced with either nontargeting shRNA vector or with either of two different individual shRNAs targeting *AGTR2* (**E**), *CRKL* (**F**), *TBX2* (**G**), and *SLC26A2* (**H**) were treated with varying concentrations of recombinant TRAIL for 24 hours. Survival as a percentage of untreated cells was determined by CellTiter-Glo Luminescent Cell Viability Assay. Representative experiments are shown (of ≥3 experiments) with each experiment performed in triplicate. Statistical significance assessed by two-way ANOVA.

Published OnlineFirst January 20, 2017; DOI: 10.1158/1541-7786.MCR-16-0234

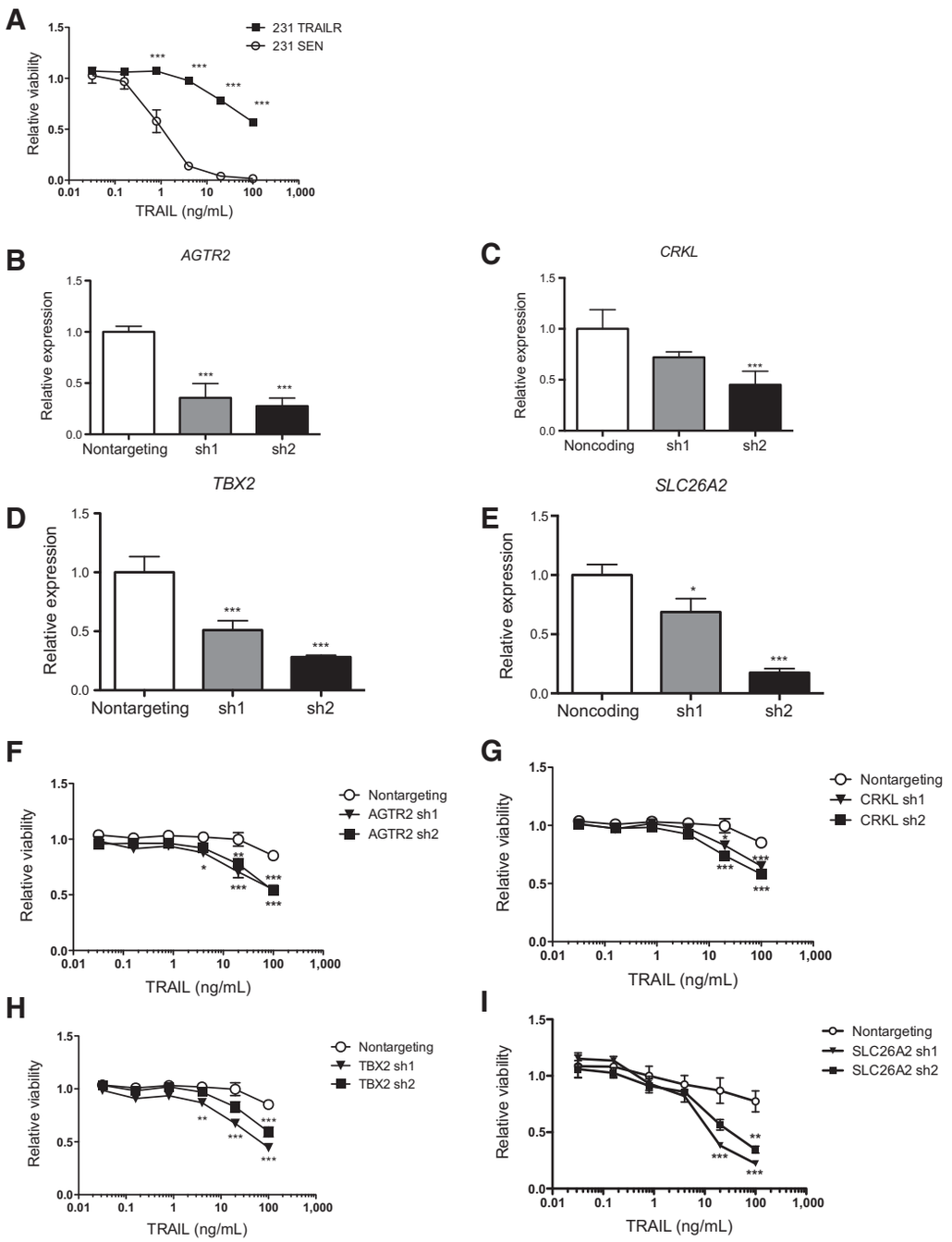

Figure 3.

AGTR2, CRKL, TBX2, and SLC26A2 mediate resistance to TRAIL in MDA-MB-231 breast cancer cells. **A,** Parental, TRAIL-sensitive MDA-MB-231 cells (231 SEN) and MDA-MB-231 cells made TRAIL resistant through long-term culture in increasing concentrations of recombinant TRAIL (231 TRAILR) were treated at indicated concentrations of recombinant TRAIL for 24 hours. Relative viability compared with untreated cells was determined by CellTiter-Glo Luminescent Cell Viability Assay. Representative experiments are shown (of ≥3 experiments) with each experiment performed in triplicate. Statistical significance assessed by two-way ANOVA with a Bonferroni posttest. **B–E,** 231 TRAILR cells were lentivirally transduced with either a control, nontargeting shRNA vector (nontargeting), or with either of two different individual shRNAs (sh1, sh2) targeting *AGTR2* (**B**), *CRKL* (**C**), *TBX2* (**D**), and *SLC26A2* (**E**). KD was determined by qRT-PCR. The expression is relative to the expression of GAPDH and was normalized to nontargeting shRNA vector-expressing cells. Representative experiments are shown (of ≥3 experiments) with each experiment performed in triplicate. Statistical significance assessed by two-way ANOVA with a Bonferroni posttest. **F–I,** 231 TRAILR cells transduced with either a control, nontargeting shRNA vector (nontargeting) or with either of two different individual shRNAs (sh1, sh2) targeting *AGTR2* (**F**), *CRKL* (**G**), *TBX2* (**H**), and *SLC26A2* (**I**) were treated with varying concentrations of recombinant TRAIL for 24 hours. Survival as a percentage of untreated cells was determined by CellTiter-Glo Luminescent Cell Viability Assay. Representative experiments are shown (of ≥3 experiments) with each experiment performed in triplicate. Statistical significance assessed by two-way ANOVA.

Published OnlineFirst January 20, 2017; DOI: 10.1158/1541-7786.MCR-16-0234

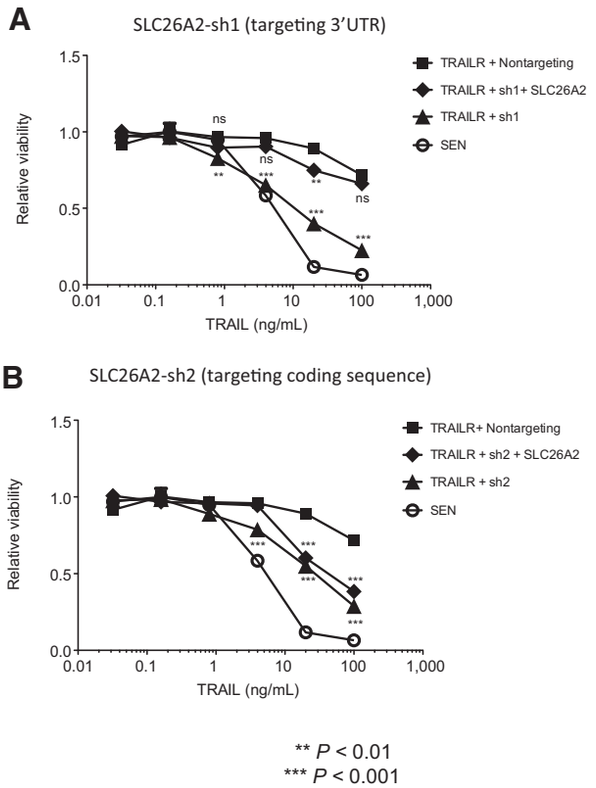

Figure 4.

TRAIL-resistant MDA-MB-231 cells are resensitized to TRAIL by KD of SLC26A2. 231 SEN and 231 TRAILR cells transduced with a nontargeting control shRNA or with shRNA 1 that targets *SLC26A2* in the 3′UTR of the gene (RES + sh1; **A**), such that the shRNA will not KD exogenous SLC26A2 or with shRNA 2 that targets *SLC26A2* in the coding region and can target both exogenous and endogenous proteins were treated with indicated concentrations of recombinant TRAIL for 24 hours (**B**). Survival as a percentage of untreated cells was determined by CellTiter-Glo Luminescent Cell Viability Assay. Representative experiments are shown (of $\geq$3 experiments) with each experiment performed in triplicate. Statistical significance assessed by two-way ANOVA with a Bonferroni posttest.

cross-referenced this data with that of our shRNA screen. This analysis showed increased *SLC26A2* expression in the MDA-MB-231-TRAILR cell line as compared with its sensitive counterpart (Fig. 5C). Interestingly, we also noted that expression of the TRAIL receptors, *DR4* and *DR5*, were decreased in the array analyses (Fig. 5C). The increase of *SLC26A2* and concomitant decrease of *DR4* and *DR5* expression in MDA-MB-231-TRAILR cells when compared to their sensitive counterparts was confirmed using qRT-PCR (Fig. 5D–F) and Western blot analysis (Fig. 5G). Importantly, there was also reduced surface protein expression of DR4 and DR5 as assessed by flow cytometry in the MDA-MB-231-TRAILR cells as compared to the SEN cells (Fig. 5H and I). These results were confirmed in the BJAB cell system, where we again observed an increase in *SLC26A2* mRNA expression and a corresponding decrease in surface protein expression of DR4 and DR5 in the BJAB-LexR cells as compared to the BJAB-wt cells (Supplementary Fig. S4A–S4C).

Because KD of SLC26A2 reversed resistance to TRAIL and because downregulation of DR4 and DR5, crucial mediators of TRAIL apoptosis, is associated with acquired TRAIL resistance, we next assessed whether TRAIL sensitivity, SLC26A2 expression, and expression of DR4 and DR5 were linked. To this end, we analyzed the expression of these receptors in MDA-MB-231-TRAILR sublines with stable SLC26A2 KD. Notably, TRAIL-resistant MDA-MB-231 cells transduced with nontargeting shRNA had approximately the same DR4 and DR5 expression as nontransduced TRAIL-resistant cells. However, in MDA-MB-231-TRAILR cells transduced with shRNAs targeting *SLC26A2*, the mRNA, protein in whole cell lysates, and surface protein levels of DR4 and DR5 were restored (Fig. 5H and I). Together, these data demonstrate that *SLC26A2* is regulating the overall levels of DR4 and DR5, and more importantly, surface levels of DR4 and DR5.

SLC26A2 expression correlates with worsened disease in human tumors

Because many tumors are known to be resistant to TRAIL, we asked whether the levels of SLC26A2 may be elevated in human tumors, as a means to induce TRAIL resistance. Indeed, numerous public gene expression datasets, spanning multiple tumor types, show a significant increase in *SLC26A2* expression in tumor as compared to normal tissue (Table 1; ref. 30–40). In addition, elevated *SLC26A2* expression correlates with metastasis or worsened prognosis in numerous tumor types (41–47). Importantly, in a cohort of 1,000 untreated breast cancer patients (taken from multiple studies using KMplot; ref. 26), high *SLC26A2* expression correlated with a significant decrease in relapse free survival and almost significant decrease in distant metastasis free survival (Fig. 6 and Supplementary Fig. S5). Together, these data demonstrate that *SLC26A2* is a marker for cancer versus normal as well as an indicator for poor prognosis in breast cancer and other cancers, and suggest that it may regulate tumor progression at least in part via its ability to mediate TRAIL resistance.

Discussion

Much enthusiasm initially surrounded the promise of TRAIL agonist therapy as a specific means to target cancers. However, the lack of anticancer activity in a significant number of patients displayed during phase II clinical trials has been disappointing (5). The last decade has revealed insight into multiple missteps that occurred with the initial TRAIL agonist therapies, most specifically because there are many routes of resistance that tumors can acquire to escape death induced by TRAIL, and it is critical to both develop strategies to circumvent resistance and identify upfront the most likely responders for successful use of TRAIL receptor–targeted therapies. Despite this new understanding, neither a successful combination therapy nor the use of biomarkers for TRAIL sensitivity, to identify the patients who are likely to benefit, have moved into clinical trials.

To find novel resistance markers and obtain a more general view of TRAIL resistance mechanisms beyond the known mechanisms that generally involve direct participants in the core TRAIL pathway, we performed a genome wide shRNA loss of function screen in TRAIL-resistant cell lines (Fig. 1). This unbiased approach allowed for the discovery of unique genes that were

Published OnlineFirst January 20, 2017; DOI: 10.1158/1541-7786.MCR-16-0234

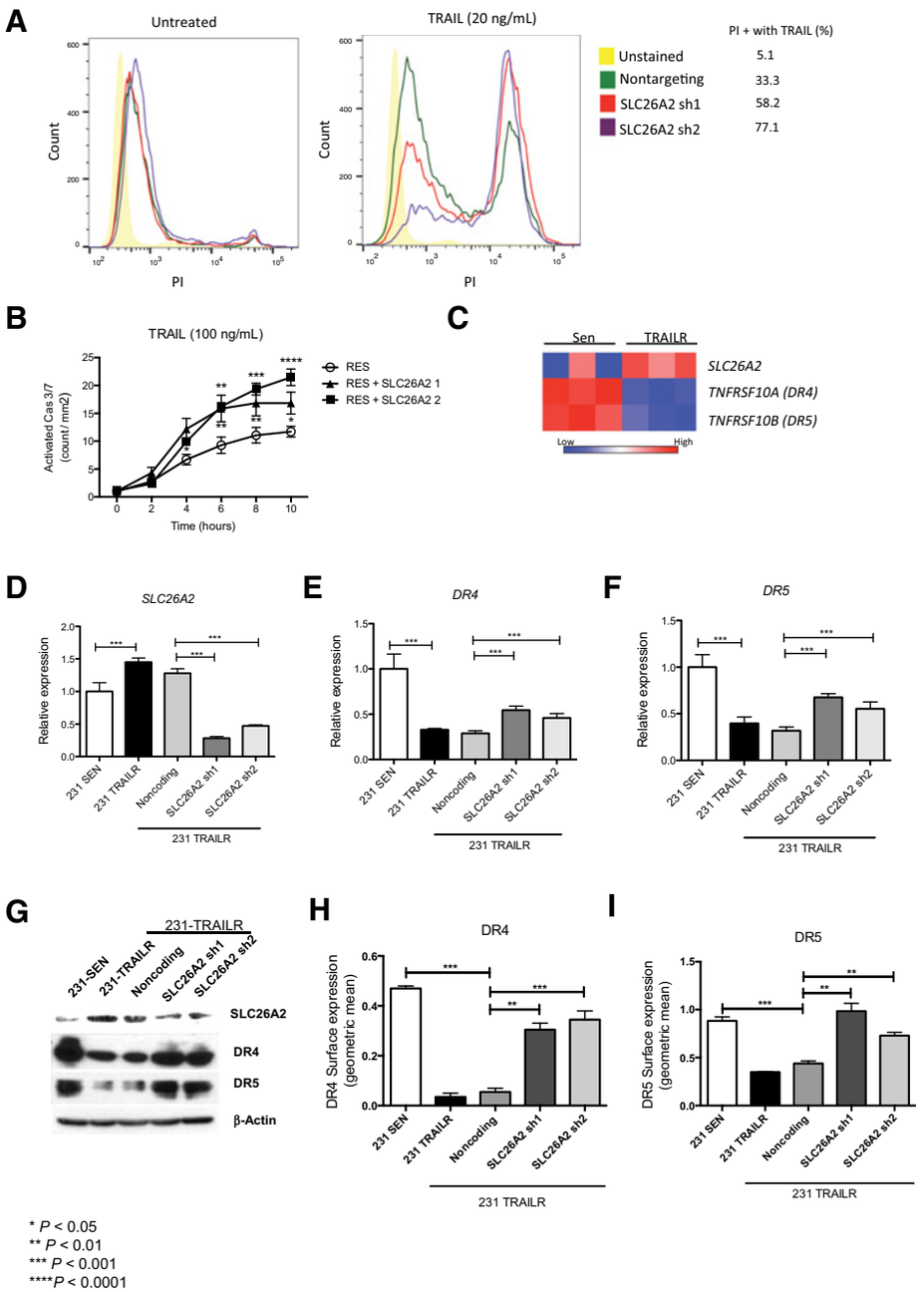

Figure 5.

SLC26A2 regulates the TRAIL receptors, DR4 and DR5, in MDA-MB-231 cells. **A,** Flow cytometry analysis in BJAB-LEXR cells with stable, lentiviral, shRNAs against *SLC26A2* or a nontargeting shRNA after 24 hours of treatment with TRAIL (20 ng/mL) to assess PI-positive cells as an indication of dead or late apoptotic cells. Representative experiment is shown (of two experiments). **B,** MDA-231 SENS and TRAILR cells plated in replicates of six were treated with TRAIL (100 ng/mL) and a green fluorogenic substrate for activated-caspase-3/7. Green fluorescence was measured every 2 hours with 100 ng/mL TRAIL by light microscopy using real-time *in vitro* imaging. Statistical significance assessed by two-way ANOVA with a Tukey posttest. A representative figure is shown (of two experiments). **C,** Triplicate samples of 231 SEN and 231 TRAILR were analyzed for RNA expression of *SLC26A2*, *DR4*, and *DR5*, using microarray analysis. The expression is presented as a heatmap relative to an average expression of a combination of constitutive housekeeping genes. RNA and protein were isolated from 231 SEN cells and 231 TRAILR cells as well as 231 TRAILR cells transduced with a nontargeting control shRNA (noncoding) or with either of two shRNA targeting *SLC26A2* (SLC26A2 sh1 and SLC26A2 sh2, respectively). mRNA expression of *SLC26A2* (**D**), *DR4* (**E**), and *DR5* (**F**) was determined by qRT-PCR. The expression is relative to the expression of *GAPDH* and was normalized to the nontargeting shRNA vector-expressing cells. Representative experiments are shown (of ≥3 experiments) with each experiment performed in triplicate. Statistical significance assessed by one-way ANOVA. Protein expression of these genes as well as β-actin was analyzed by Western blot analysis as shown in **G**. Surface expression of DR4 and DR5 was analyzed by flow cytometry as depicted in **H** and **I**, respectively. Representative experiments are shown (of ≥3 experiments). Statistical significance assessed by one-way ANOVA.

Published OnlineFirst January 20, 2017; DOI: 10.1158/1541-7786.MCR-16-0234

Table 1. *SLC26A2* overexpression is correlated with worsened disease

Tumor type	Differential expression	Fold change	*P*	Dataset
Breast	Metastatic event at 1 year vs. no event at 1 year	2.282	9.88E−10	Minn Breast 2
Breast	Metastatic site vs. primary site	2.485	0.005	Weigelt Breast
Brain	Glioblastoma dead at 5 years vs. alive	2.531	6.02E−4	Nutt Brain
Lung	Lung adenocarcioma - advanced N stage	2.125	0.001	Beer Lung
Breast	Ductal breast carcinoma- ERBB2/ER/PR negative vs. positive	5.313	5.75E−6	Richardson Breast 2
Breast	Invasive ductal breast carcinoma stroma vs. normal	2.214	8.23E−5	Karnoub Breast
Colon	Colon adenocarcinoma dead at 1 year vs. alive	2.695	0.003	TCGA Colorectal
Brain	Glioblastoma vs. normal	2.002	6.38E−18	Sun Brain
Lymphoma	Anaplastic large cell lymphoma vs. normal	5.641	2.79E−8	Piccaluga Lymphoma
Lymphoma	Angioimmunoblastiv T-cell lymphoma vs. normal	3.689	5.32E−8	Piccaluga Lymphoma
Lymphoma	Unspecified peripheral T-cell lymphoma vs. normal	3.489	6.22E−13	Piccaluga Lymphoma
Ovarian	Ovarian clear cell adenocarcinoma vs. normal	2.353	8.41E−4	Lu Ovarain
Prostate	Prostatic intraepithelial neoplasia epithelia vs. normal	3.646	1.53E−4	Tomlins Prostate
Liver	Hepatocellular carcinoma vs. normal	3.239	5.64E−5	Wurmbach Liver
Renal	Nonhereditary clear cell renal carcinoma vs. normal	2.371	6.45E−7	Beroukhim Renal
Melanoma	Skin basal cell carcinoma vs. normal	2.337	2.15E−4	Riker Melanoma
Melanoma	Metastaic site vs. primary site	2.079	5.01E−5	Xu Melanoma
Renal	Renal Wilms tumor vs. normal	2.210	0.004	Yusenko Renal
Brain	Glioblastoma vs. normal	2.328	5.46E−5	Murat Brain
Brain	Anaplastic oligodendroglioma vs. normal	2.384	1.86E−5	French Brain

not previously linked to TRAIL signaling or drug resistance in general. Using gene-specific shRNAs in two different cell line systems (encompassing different tumor types), we confirmed that downregulation of four specific genes resensitize resistant cell lines to TRAIL agonist therapy (*AGTR2*, *CRKL*, *TBX2*, and *SLC26A2*; Figs. 2 and 3). Importantly, none of these genes are involved in the core TRAIL signaling pathway, nor are they general regulators of apoptosis, emphasizing the ability of the genome wide unbiased screen to find new unanticipated regulators of TRAIL resistance.

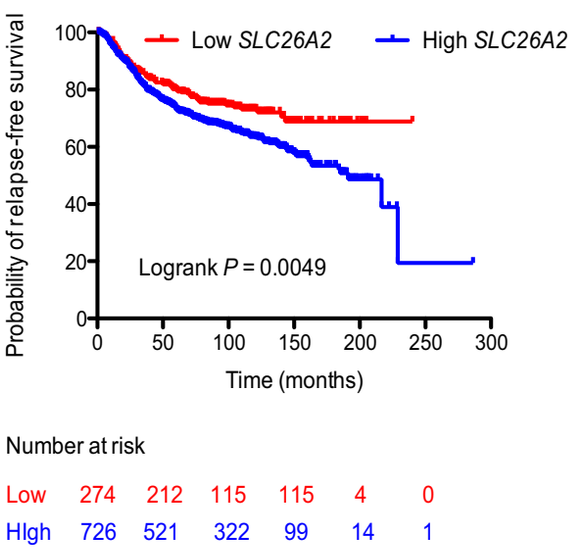

Figure 6.
SLC26A2 expression correlates with worsened prognosis in breast cancer. With the use of KMplot (53), 1,000 untreated breast cancer patients were divided into two groups with either high *SLC26A2* expression (approximately top 3 quartiles) or low *SLC26A2* expression (approximately bottom quartile). Patients with high *SLC26A2* expression have a decreased probability of relapse-free survival.

Interestingly, we discovered a connection between these seemingly unrelated TRAIL resistance genes discovered in our screen. This connection was discovered by performing genome-scale integrated-analysis of gene networks (GIANT) across all tissues (29). Restricting the analysis to highly significant relationships (relationship confidence >0.5) with a maximum number of 20 genes to form the network, we found that all four genes are connected (Fig. 7A) through a functional network that is significantly associated with a number of pathways, processes, and diseases, the majority of which are relevant to cancer (Supplementary Table S1). Interestingly, microarray analysis of BJAB WT and LEXR TRAIL-treated samples as well as MDA-231 SENS and TRAILR TRAIL-treated samples, followed by GSEA of significantly changed genes reveals that a number of similar pathways are enriched (Supplementary Table S2 and S3). In particular, the ErbB/EGFR signaling pathway (or KEGG pathways that contain large portions of this pathway) is significantly associated with the functional network created between the four confirmed genes, as well as in the microarray analyses from both the BJAB and MDA-MB-231 cell lines (Fig. 7B and C). These results strongly suggest that ErbB signaling may be relevant for TRAIL resistance. Importantly, downregulation of ErbB/EGFR has been previously associated with increasing TRAIL sensitivity. Specifically, decreased expression of ErbB with either trastuzumab or antisense oligodeoxynucleotides sensitizes ErbB overexpressing breast and ovarian cells to TRAIL-mediated apoptosis (48). Additional studies have mechanistically linked EGFR to TRAIL resistance via the Bcl-2 family member myeloid cell leukemia 1 (Mcl-1; ref. 49) as well as cytochrome C release and caspase-3–like activation (50).

Although numerous potential TRAIL-resistant genes were identified in our screen, here we focused on the anion exchange channel *SLC26A2*. We demonstrate that knocking down this gene, which has never been previously been implicated in cancer drug sensitivity, significantly resensitizes resistant cells to TRAIL agonist therapy in both lymphoma cells and breast cancer cells. The effect was not a general proapoptotic effect as apoptosis induced by other apoptosis-inducing agents were not affected (Fig. S3). Moreover, when SLC26A2 was reintroduced into cells with knocked down SLC26A2, the cells became

Published OnlineFirst January 20, 2017; DOI: 10.1158/1541-7786.MCR-16-0234

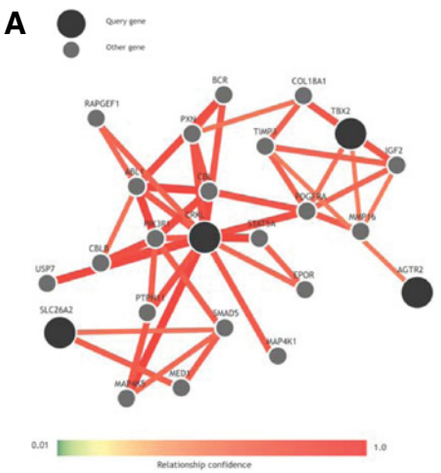

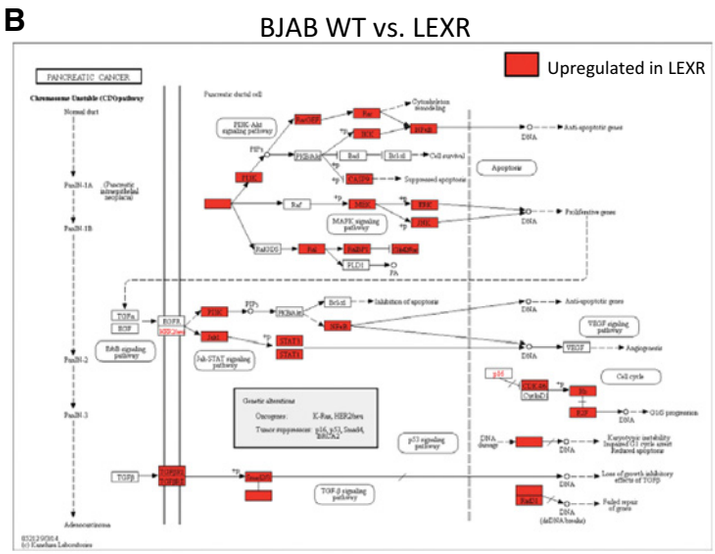

FIGF	JAK1
KRAS	CDK6
RALA	TGFBR1
PIK3CA	E2F3
RALB	RAC1
ARHGEF6	CASP9
PIK3R3	STAT1
PIK3CB	PIK3CG
MAPK10	CDK4
MAPK9	MAPK1
RB1	TP53
NFKB1	TGFBR2
CHUK	RAD51
MAP2K1	BRCA2
SMAD2	CDC42
SMAD4	SMAD3
RALBP1	MAPK8
PIK3R1	STAT3

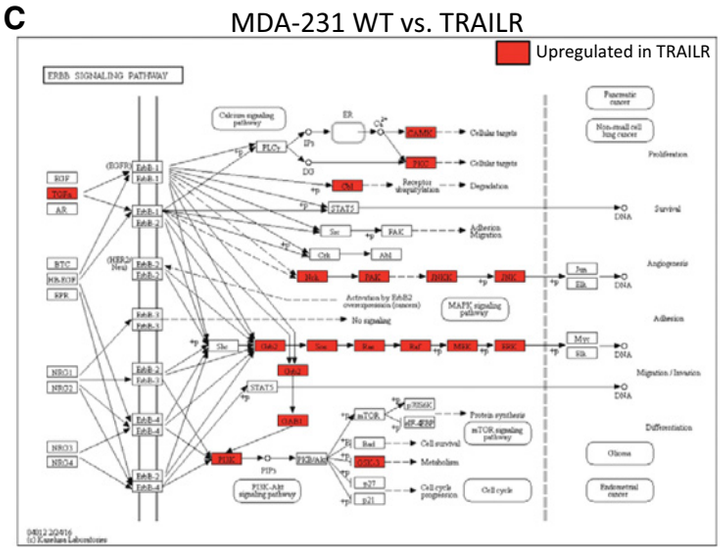

KRAS	PIK3CB
PAK2	CAMK2D
MAP2K4	MAP2K1
PIK3R1	SOS2
MAPK8	GAB1
NCK2	PRKCA
SOS1	RAF1
PIK3CA	
NCK1	
TGFA	
PIK3R3	
NRAS	
MAPK9	
GRB2	
PIK3CG	
GSK3B	
CBL	
MAPK1	

Figure 7.

Pathway analysis identifies a functional network between *AGTR2*, *CRKL*, *TBX2*, and *SLC26A2*. **A,** Use of GIANT (29) with *AGTR2*, *CRKL*, *TBX2*, and *SLC26A2* as inputs analyzed across all tissue types (relationship confidence > 0.5 and max number of genes set to 20). **B** and **C,** Microarray analyses were performed on mRNA from BJAB WT and LEXR samples (**B**) and MDA-231 SENS and TRAILR samples after treatment with TRAIL (100 ng/mL), followed by GSEA analysis (**C**). **B,** The KEGG pancreatic signaling pathway (consisting mostly of ErbB/EGFR signaling pathways) is displayed with core genes upregulated (enriched) in the trail-treated BJAB-LEXR samples as compared with TRAIL-treated BJAB-WT samples in red. **C,** The KEGG ErbB signaling pathway is displayed with core genes upregulated (enriched) in the TRAIL-treated MDA-231 TRAILR samples as compared with the TRAIL-treated MDA-231 SENS samples.

resensitized to TRAIL-induced apoptosis indicating that expression of this gene is both necessary and sufficient to confer selective TRAIL resistance (Fig. 4). Expression of SLC26A2 led to downregulation of the death receptors DR4 and DR5, suggesting a plausible mechanism by which SLC26A2 counteracts TRAIL-induced apoptosis (Fig. 5C-I).

Although SLC26A2 has not previously been associated with pro-tumorigenic phenotypes, examination of tumor microarray datasets reveals increased expression of *SLC26A2* in tumor tissue as compared with normal tissue across multiple tumor types including Wilms tumor, glioblastoma, lymphoma, ovarian, breast, hepatocellular, skin, and renal carcinoma (Table 1; refs. 30–47). Furthermore, other datasets show a correlation between elevated *SLC26A2* expression and worsened prognosis or metastasis, particularly in glioblastoma, melanoma, breast, and lung cancer (Table 1 and Fig. 6). As SLC26A2 is understudied, there are no known specific inhibitors to block this channel, although other anion channel inhibitors have already moved into clinical trials for the treatment of cancer, suggesting that targeting SLC26A2 may be feasible (51).

TRAIL receptor-targeted therapy has so far been disappointing in the clinic, underscoring how inadequate understanding of potential resistance mechanisms prior to starting clinical studies can contribute to the failure of targeted therapies (52). Innovative, genome-wide studies, such as that described here, provide a way to gain a comprehensive understanding of potential resistance mechanisms that cancer cells can employ to evade TRAIL-induced apoptosis, or to evade apoptosis induced by other targeted agents. In addition, these approaches can also uncover strategic combinational therapies that could synergize with TRAIL agonist therapies in clinic. Although the majority of patients seem unresponsive to TRAIL monotherapies, survival curves indicate that a small percentage of patients do benefit. Development of a panel of strategic molecular biomarkers using the approaches described here may allow for a way to better identify those patients who may benefit from TRAIL receptor-targeted therapies.

Disclosure of Potential Conflicts of Interest

No potential conflicts of interest were disclosed.

Authors' Contributions

Conception and design: L.Y. Dimberg, K. Behbakht, A. Thorburn, H.L. Ford
Development of methodology: L.Y. Dimberg, A.-C. Tan, H.L. Ford
Acquisition of data (provided animals, acquired and managed patients, provided facilities, etc.): L.Y. Dimberg, C.G. Towers, K. Behbakht, T.J. Hotz, C.C. Porter, A.-C. Tan
Analysis and interpretation of data (e.g., statistical analysis, biostatistics, computational analysis): L.Y. Dimberg, C.G. Towers, J. Kim, A.-C. Tan, H.L. Ford
Writing, review, and/or revision of the manuscript: L.Y. Dimberg, C.G. Towers, K. Behbakht, J. Kim, C.C. Porter, A.-C. Tan, A. Thorburn, H.L. Ford
Administrative, technical, or material support (i.e., reporting or organizing data, constructing databases): S. Fosmire
Study supervision: L.Y. Dimberg, H.L. Ford

Acknowledgments

We gratefully acknowledge the substantial contribution of Joshua Cabrera in the acquisition, analysis, and interpretation of the data presented in this publication. Because Mr. Cabrera passed away before this article was written, listing him as a co-author is not consistent with the policies of the journal. We would also like to thank Jackie Thorburn and Lubna Qamar for technical assistance with experiments performed in this manuscript. Finally, we would like to acknowledge Rani Powers for her insight into GIANT pathway analysis.

Grant Support

This work was supported by NIH GrantCA124545 (to A. Thorburn, K. Behbakht, and H. Ford), Department of Defense (DOD) postdoctoral fellowship BC093627 and Swedish Research Council postdoctoral fellowship 2009-618 (to L. Dimberg), DOD Ovarian Cancer Idea AwardOC06143 (to K. Behbakht), and the Bioscience Discovery and Evaluation Grant (to A. Thorburn, K. Behbakht, and H. Ford). C. Towers was funded by the UC Denver AMC Molecular Biology Program T32 training grant, NIH-RO1 Diversity Supplement to R01-CA157790, and the UNCF/MERCK Graduate Fellowship. The flow cytometry, functional genomics and genomics shared resource were funded by the Cancer Center support grant (CA046934).

The costs of publication of this article were defrayed in part by the payment of page charges. This article must therefore be hereby marked *advertisement* in accordance with 18 U.S.C. Section 1734 solely to indicate this fact.

Received July 13, 2016; revised November 16, 2016; accepted November 29, 2016; published OnlineFirst January 20, 2017.

References

1. Pitti RM, Marsters SA, Ruppert S, Donahue CJ, Moore A, Ashkenazi A. Induction of apoptosis by Apo-2 ligand, a new member of the tumor necrosis factor cytokine family. J Biol Chem 1996;271:12687–90.
2. Wiley SR, Schooley K, Smolak PJ, Din WS, Huang CP, Nicholl JK, et al. Identification and characterization of a new member of the TNF family that induces apoptosis. Immunity 1995;3:673–82.
3. Ashkenazi A, Pai RC, Fong S, Leung S, Lawrence DA, Marsters SA, et al. Safety and antitumor activity of recombinant soluble Apo2 ligand. J Clin Invest 1999;104:155–62.
4. Walczak H, Miller RE, Ariail K, Gliniak B, Griffith TS, Kubin M, et al. Tumoricidal activity of tumor necrosis factor-related apoptosis-inducing ligand *invivo*. Nat Med 1999;5:157–63.
5. Dimberg LY, Anderson CK, Camidge R, Behbakht K, Thorburn A, Ford HL. On the TRAIL to successful cancer therapy? Predicting and counteracting resistance against TRAIL-based therapeutics. Oncogene 2013;32:1341–50.
6. von Pawel J, Harvey JH, Spigel DR, Dediu M, Reck M, Cebotaru CL, et al. Phase II trial of mapatumumab, a fully human agonist monoclonal antibody to tumor necrosis factor-related apoptosis-inducing ligand receptor 1 (TRAIL-R1), in combination with paclitaxel and carboplatin in patients with advanced non-small-cell lung cancer. Clin Lung Cancer 2014;15:188–96.
7. Trivedi R, Mishra DP. Trailing TRAIL resistance: novel targets for TRAIL sensitization in cancer cells. Front Oncol 2015;5:69.
8. Gump JM, Staskiewicz L, Morgan MJ, Bamberg A, Riches DW, Thorburn A. Autophagy variation within a cell population determines cell fate through selective degradation of Fap-1. Nat Cell Biol 2014;16:47–54.
9. Graff JR, Konicek BW, Carter JH, Marcusson EG. Targeting the eukaryotic translation initiation factor 4E for cancer therapy. Cancer Res 2008;68:631–4.
10. Fan S, Li Y, Yue P, Khuri FR, Sun SY. The eIF4E/eIF4G interaction inhibitor 4EGI-1 augments TRAIL-mediated apoptosis through c-FLIP Down-regulation and DR5 induction independent of inhibition of cap-dependent protein translation. Neoplasia 2010;12:346–56.
11. Johnson TR, Stone K, Nikrad M, Yeh T, Zong WX, Thompson CB, et al. The proteasome inhibitor PS-341 overcomes TRAIL resistance in Bax and caspase 9-negative or Bcl-xL overexpressing cells. Oncogene 2003;22:4953–63.

12. Wagner KW, Punnoose EA, Januario T, Lawrence DA, Pitti RM, Lancaster K, et al. Death-receptor O-glycosylation controls tumor-cell sensitivity to the proapoptotic ligand Apo2L/TRAIL. Nat Med 2007;13:1070–7.
13. Yang JK. FLIP as an anti-cancer therapeutic target. Yonsei Med J 2008;49: 19–27.
14. Cummins JM, Kohli M, Rago C, Kinzler KW, Vogelstein B, Bunz F. X-linked inhibitor of apoptosis protein (XIAP) is a nonredundant modulator of tumor necrosis factor-related apoptosis-inducing ligand (TRAIL)-mediated apoptosis in human cancer cells. Cancer Res 2004;64:3006–8.
15. Ng CP, Bonavida B. X-linked inhibitor of apoptosis (XIAP) blocks Apo2 ligand/tumor necrosis factor-related apoptosis-inducing ligand-mediated apoptosis of prostate cancer cells in the presence of mitochondrial activation: sensitization by overexpression of second mitochondria-derived activator of caspase/direct IAP-binding protein with low pl (Smac/DIABLO). Mol Cancer Ther 2002;1:1051–8.
16. Menke C, Bin L, Thorburn J, Behbakht K, Ford HL, Thorburn A. Distinct TRAIL resistance mechanisms can be overcome by proteasome inhibition but not generally by synergizing agents. Cancer Res 2011;71:1883–92.
17. Porter CC, Kim J, Fosmire S, Gearheart CM, van Linden A, Baturin D, et al. Integrated genomic analyses identify WEE1 as a critical mediator of cell fate and a novel therapeutic target in acute myeloid leukemia. Leukemia 2012;26:1266–76.
18. Menke C, Goncharov T, Qamar L, Korch C, Ford HL, Behbakht K, et al. TRAIL receptor signaling regulation of chemosensitivity *invivo* but not *invitro*. PLoS One 2011;6:e14527.
19. Kim J, Tan AC. BiNGS!SL-seq: a bioinformatics pipeline for the analysis and interpretation of deep sequencing genome-wide synthetic lethal screen. Methods Mol Biol 2012;802:389–98.
20. Spreafico A, Tentler JJ, Pitts TM, Tan AC, Gregory MA, Arcaroli JJ, et al. Rational combination of a MEK inhibitor, selumetinib, and the Wnt/calcium pathway modulator, cyclosporin A, in preclinical models of colorectal cancer. Clin Cancer Res 2013;19:4149–62.
21. Sullivan KD, Padilla-Just N, Henry RE, Porter CC, Kim J, Tentler JJ, et al. ATM and MET kinases are synthetic lethal with nongenotoxic activation of p53. Nat Chem Biol 2012;8:646–54.
22. Casas-Selves M, Kim J, Zhang Z, Helfrich BA, Gao D, Porter CC, et al. Tankyrase and the canonical Wnt pathway protect lung cancer cells from EGFR inhibition. Cancer Res 2012;72:4154–64.
23. Langmead B, Trapnell C, Pop M, Salzberg SL. Ultrafast and memory-efficient alignment of short DNA sequences to the human genome. Genome Biol 2009;10:R25.
24. Robinson MD, McCarthy DJ, Smyth GK. edgeR: a Bioconductor package for differential expression analysis of digital gene expression data. Bioinformatics 2010;26:139–40.
25. Bonafe L, Hastbacka J, de la Chapelle A, Campos-Xavier AB, Chiesa C, Forlino A, et al. A novel mutation in the sulfate transporter gene SLC26A2 (DTDST) specific to the Finnish population causes de la Chapelle dysplasia. J Med Genet 2008;45:827–31.
26. Gyorffy B, Lanczky A, Eklund AC, Denkert C, Budczies J, Li Q, et al. An online survival analysis tool to rapidly assess the effect of 22,277 genes on breast cancer prognosis using microarray data of 1,809 patients. Breast Cancer Res Treat 2010;123:725–31.
27. Irizarry RA, Hobbs B, Collin F, Beazer-Barclay YD, Antonellis KJ, Scherf U, et al. Exploration, normalization, and summaries of high density oligonucleotide array probe level data. Biostatistics 2003;4:249–64.
28. Subramanian A, Tamayo P, Mootha VK, Mukherjee S, Ebert BL, Gillette MA, et al. Gene set enrichment analysis: a knowledge-based approach for interpreting genome-wide expression profiles. Proc Natl Acad Sci U S A 2005;102:15545–50.
29. Greene CS, Krishnan A, Wong AK, Ricciotti E, Zelaya RA, Himmelstein DS, et al. Understanding multicellular function and disease with human tissue-specific networks. Nat Genet 2015;47:569–76.
30. Karnoub AE, Dash AB, Vo AP, Sullivan A, Brooks MW, Bell GW, et al. Mesenchymal stem cells within tumour stroma promote breast cancer metastasis. Nature 2007;449:557–63.
31. Sun L, Hui AM, Su Q, Vortmeyer A, Kotliarov Y, Pastorino S, et al. Neuronal and glioma-derived stem cell factor induces angiogenesis within the brain. Cancer Cell 2006;9:287–300.
32. Piccaluga PP, Agostinelli C, Califano A, Rossi M, Basso K, Zupo S, et al. Gene expression analysis of peripheral T cell lymphoma, unspecified, reveals distinct profiles and new potential therapeutic targets. J Clin Invest 2007;117:823–34.
33. Lu KH, Patterson AP, Wang L, Marquez RT, Atkinson EN, Baggerly KA, et al. Selection of potential markers for epithelial ovarian cancer with gene expression arrays and recursive descent partition analysis. Clin Cancer Res 2004;10:3291–300.
34. Tomlins SA, Mehra R, Rhodes DR, Cao X, Wang L, Dhanasekaran SM, et al. Integrative molecular concept modeling of prostate cancer progression. Nat Genet 2007;39:41–51.
35. Wurmbach E, Chen YB, Khitrov G, Zhang W, Roayaie S, Schwartz M, et al. Genome-wide molecular profiles of HCV-induced dysplasia and hepatocellular carcinoma. Hepatology 2007;45:938–47.
36. Beroukhim R, Brunet JP, Di Napoli A, Mertz KD, Seeley A, Pires MM, et al. Patterns of gene expression and copy-number alterations in von-Hippel Lindau disease-associated and sporadic clear cell carcinoma of the kidney. Cancer Res 2009;69:4674–81.
37. Riker AI, Enkemann SA, Fodstad O, Liu S, Ren S, Morris C, et al. The gene expression profiles of primary and metastatic melanoma yields a transition point of tumor progression and metastasis. BMC Med Genomics 2008;1:13.
38. Yusenko MV, Kuiper RP, Boethe T, Ljungberg B, van Kessel AG, Kovacs G. High-resolution DNA copy number and gene expression analyses distinguish chromophobe renal cell carcinomas and renal oncocytomas. BMC Cancer 2009;9:152.
39. Murat A, Migliavacca E, Gorlia T, Lambiv WL, Shay T, Hamou MF, et al. Stem cell-related "self-renewal" signature and high epidermal growth factor receptor expression associated with resistance to concomitant chemoradiotherapy in glioblastoma. J Clin Oncol 2008;26:3015–24.
40. French PJ, Swagemakers SM, Nagel JH, Kouwenhoven MC, Brouwer E, van der Spek P, et al. Gene expression profiles associated with treatment response in oligodendrogliomas. Cancer Res 2005;65:11335–44.
41. Minn AJ, Gupta GP, Siegel PM, Bos PD, Shu W, Giri DD, et al. Genes that mediate breast cancer metastasis to lung. Nature 2005;436:518–24.
42. Weigelt B, Glas AM, Wessels LF, Witteveen AT, Peterse JL, van't Veer LJ. Gene expression profiles of primary breast tumors maintained in distant metastases. Proc Natl Acad Sci U S A 2003;100:15901–5.
43. Nutt CL, Mani DR, Betensky RA, Tamayo P, Cairncross JG, Ladd C, et al. Gene expression-based classification of malignant gliomas correlates better with survival than histological classification. Cancer Res 2003;63:1602–7.
44. Beer DG, Kardia SL, Huang CC, Giordano TJ, Levin AM, Misek DE, et al. Gene-expression profiles predict survival of patients with lung adenocarcinoma. Nat Med 2002;8:816–24.
45. Richardson AL, Wang ZC, De Nicolo A, Lu X, Brown M, Miron A, et al. X chromosomal abnormalities in basal-like human breast cancer. Cancer Cell 2006;9:121–32.
46. The Cancer Genome Atlas Network. Comprehensie molecular characterization of human colon and rectal cancer. Nature 2012;487:330–7.
47. Xu L, Shen SS, Hoshida Y, Subramanian A, Ross K, Brunet JP, et al. Gene expression changes in an animal melanoma model correlate with aggressiveness of human melanoma metastases. Mol Cancer Res 2008;6:760–9.
48. Cuello M, Ettenberg SA, Clark AS, Keane MM, Posner RH, Nau MM, et al. Down-regulation of the erbB-2 receptor by trastuzumab (herceptin) enhances tumor necrosis factor-related apoptosis-inducing ligand-mediated apoptosis in breast and ovarian cancer cell lines that overexpress erbB-2. Cancer Res 2001;61:4892–900.
49. Henson ES, Gibson EM, Villanueva J, Bristow NA, Haney N, Gibson SB. Increased expression of Mcl-1 is responsible for the blockage of TRAIL-induced apoptosis mediated by EGF/ErbB1 signaling pathway. J Cell Biochem 2003;89:1177–92.
50. Gibson EM, Henson ES, Haney N, Villanueva J, Gibson SB. Epidermal growth factor protects epithelial-derived cells from tumor necrosis factor-related apoptosis-inducing ligand-induced apoptosis by inhibiting cytochrome c release. Cancer Res 2002;62:488–96.
51. Lang F, Stournaras C. Ion channels in cancer: future perspectives and clinical potential. Philos Trans R Soc Lond B Biol Sci 2014;369:20130108.
52. Lemke J, von Karstedt S, Zinngrebe J, Walczak H. Getting TRAIL back on track for cancer therapy. Cell Death Differ 2014;21:1350–64.
53. Gyorffy B, Surowiak P, Budczies J, Lanczky A. Online survival analysis software to assess the prognostic value of biomarkers using transcriptomic data in non-small-cell lung cancer. PLoS One 2013;8:e82241.

Published OnlineFirst January 20, 2017; DOI: 10.1158/1541-7786.MCR-16-0234

Molecular Cancer Research

A Genome-Wide Loss-of-Function Screen Identifies SLC26A2 as a Novel Mediator of TRAIL Resistance

Lina Y. Dimberg, Christina G. Towers, Kian Behbakht, et al.

Mol Cancer Res 2017;15:382-394. Published OnlineFirst January 20, 2017.